iJET International Journal of Engineering & Technology
CENTRE OF PROFESSIONAL RESEARCH PUBLICATIONS
ISSN 2049-3444

International Journal of Engineering and Technology Volume 3 No. 8, August, 2013

A Computational Method for Prescribing Seasonal Nitrate Loads on Farmlands to Preserve Underground Freshwater Resources

Fashanu T. A., Olunloyo V.O.S., Ibidapo-Obe O.
Department of Systems Engineering; University of Lagos, Nigeria

ABSTRACT

To date, widespread proliferation of nitrogen based manure in support of arable agricultural production has continued with little or no control. This trend is in spite of increase in medical pointers to the carcinogenic effects of excess nitrates in human systems. Small and large scale nitrate regulation policies on farmlands are fast evolving, especially in modern European agricultural communities. This is not true of many developing countries where agricultural production is the mainstay of the economy. Such economies are characterized with rudimentary level of infrastructure in rural areas. In such cases, scarcely treated groundwater remains the only reliable source of water supply for domestic and other uses. As a means of monitoring and regulating the risk to aquifers in this zone, a mathematical model is developed based on the Space-Time Conservation Element/Solution Element (CE/SE) numerical scheme for estimating the breakthrough curves of nitrate in aquifers in the neighborhood of farmlands. The model accommodates both the seasonal nature of fertilizer application as well as the stratification in geological log. Such curves enable the prescription of seasonal nitrate loads for specified well depths for various categories of water use in such environment (e.g. domestic use, irrigation etc). The developed computational scheme can be generalized to handle pastoral farming and other industrial/nuclear contaminants.

Keywords: *Contaminant Transport, Numerical Simulation, Freshwater Aquifer, Agriculture, Safe Nitrate Loads*

1. INTRODUCTION

The World Health Organization (WHO) recently sounded the alarm of an impending freshwater crisis in the year 2025 especially in sub-Saharan Africa and other developing countries. Their conclusion was based on an assessment of the rudimentary status of water infrastructure, the sanitary and hygiene conditions, as well as the absence of concise water security measures in these countries. In most of such cases, agricultural production remains the mainstay of the economy, and improved agricultural production usually means small to medium scale farming with fertilizer, pesticide and herbicide applications. Other forms of production may include mining, and refining operations that are predominantly located in the rural areas. In these environments, excess manure, agricultural runoff and mine wastes often constitute major threat to the groundwater systems Liu et al (2012). Ironically, majority of the rural population live in such areas where groundwater is the only reliable source of domestic water supply and where chemical treatment of domestic water supply is not usually available. This constitutes a health hazard for the present generation as well as danger to the water security and financial burden for the treatment of safe water to future generations.

The problems outlined above have informed the need to monitor the use of fertilizer and other toxic agricultural inputs in the neighborhood of groundwater systems. In most developed economies, stringent policies are evolving to regulate the use of nitrogen based manure on farmlands. This is recently exemplified in the United Kingdom by the nitrate directives of the department for environment, food and rural affairs. Unfortunately, this practice has not been fully embraced in most developing countries and less so in Nigeria where large scale and subsistence agricultural practice has led to the establishment of a National Fertilizer Company. To be sure, recent studies show that Nigeria ranks amongst the leading consumer of nitrogen based fertilizer in the world on a per acre basis. This is shown in Figure 1. Also, the ongoing tripartite agreement between the World Bank, Federal Government, and some states in Nigeria to boost agricultural production through the Federal Agricultural Development and Management Authority (FADAMA) project is another pointer to the continued use of nitrate fertilizers in agric production.

A study carried out after merely a decade of fertilizer use in the region revealed that more than half of water wells sampled in most Nigerian villages have nitrate concentration in excess of the 10ppm WHO benchmark (Langenegger, 1981). According to Kaown et al (2009) nitrate is hazardous when its concentration exceeds certain level in drinking water. It is converted to nitrite in the stomach by some bacteria. Nitrite extricates oxygen from hemoglobin in human blood to induce an oxygen deficient medical condition known as methaemoglobinaemia in babies. This often leads to high infant mortality as shown in Figure 2. Other forms of medical complications that can be traced to excess nitrate in drinking water include gastric ulcer, blood cancer and ultimately death Young et al (1995).

This work develops a computational model for estimating the concentration profiles of agricultural and allied contaminants in natural groundwater reservoirs, based on the history of application of contaminants on the topsoil and the hydro-geological log of the neighboring aquifer. This model can serve as an inference engine for an expert system that determines the optimum depth to nitrate safe water in localities. It can also be used to determine well depths for other categories of water applications such as irrigation and washing. Ultimately; it specifies optimum seasonal loads of nitrate fertilizer that can be applied on the topsoil without endangering the resident groundwater resources and informs policies for watershed management.

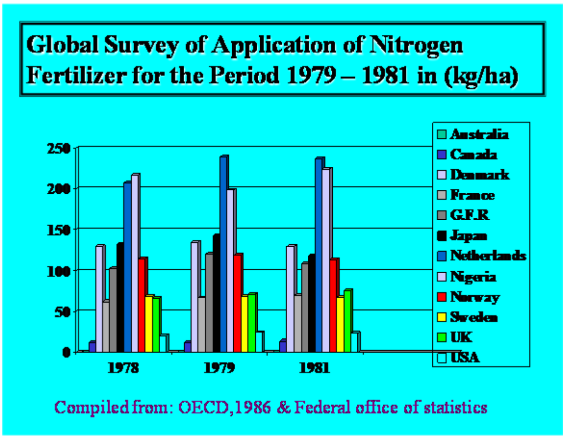

Figure 1

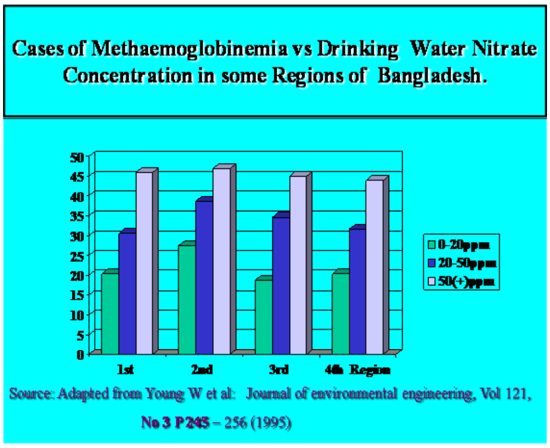

Figure 2

Generally, contaminant hydrology models often derive from operational techniques and the well known hydro dispersive scheme that combines mass and momentum transport in porous media. In this case, the mathematical physics of aqueous contaminant transport in geological reservoirs is combined with physically realistic boundary condition to simulate the concentration history of nitrate in unsaturated aquifers. In application, the model also accounts for stratification and other non-linear discontinuities characterizing the interface between hydro geological formations in freshwater aquifers. Conventional numerical methods are known to exhibit various types of pathologies at such boundaries. In addition, analytical solution of the contaminant evolution equations are likely to be quite rigorous.

Therefore, we present a simplified one dimensional Space-Time Conservation Element/Solution Element (CE/SE) numerical solution of the nitrate evolution equation. The CE/SE scheme was originally developed for computational aero-acoustic problems due to its special ability to handle physical discontinuity. By considering some of the well known hydro-geological basins and formations in Nigeria, the CE/SE computational model is applied to simulate the breakthrough curves of nitrogen-based contaminants in some homogeneous and heterogeneous freshwater aquifers. Simulations are performed in an Object Oriented Programming (OOP) environment interfaced with Matlab R2008a environment.

2. BASIC CONCEPTS OF GROUNDWATER CONTAMINANT HYDROLOGY

Microscopic model or percolation theory was the earliest model applied to model transport in porous media. It considers the dynamics of chemical specie based on individual pores of the porous media and uses stochastic (i.e. random movement) analysis to describe the overall transport. Pioneering works using the microscopic model include Ekkehard (1998), and Guler et al (2004). Essentially, these works describe the boundaries of an aquifer as an infinite network of interconnected pores of various sizes that can further be described in physical terms as skeletal conglomerate of solid part with variable porosity and permeability.

On the other hand, formulation of hydro-dispersive transfer in porous medium is based on the realization that the overall transport consists of two coupled mechanisms viz: flow and transport. Flow is due to the presence of a non-zero velocity field within a Representative Elementary Volume (REV). In the context of contaminant hydrology, the velocity field is induced either by a gravitational field (i.e. advection), or by density gradient (i.e. convection). In contrast, transport within a REV derives from processes such as diffusion, dispersion, decay, and sorption. A critical review of the two models is presented in Jack (2000). Notable works that are based on the hydro-dispersive model include Abbas and Booker (1999) as well as Park et al (2004). They adopted the concept of dual porosity to resolve contaminants flow in a geological medium into two major zones, namely momentum transport zone, coupled with a region of other transport processes. Essentially, the evolution equation to be solved in order to simulate these combined processes is the parabolic system of partial differential equations in two or more spatial dimensions, complemented by the appropriate physical initial and boundary conditions.

3. MATHEMATICAL PHYSICS OF NITRATE TRANSPORT IN AQUIFERS

Three principal processes namely advection, dispersion and reaction describe the concentration history $C_{(y,z,t)}$ of a given aqueous contaminant in a two spatial dimensional freshwater aquifer. These processes are combined with sorption and retardation phenomena to derive the governing evolution equation as:

$$\frac{\partial C}{\partial t}+\frac{V_z}{R_z}\frac{\partial C}{\partial z}+\frac{V_y}{R_y}\frac{\partial C}{\partial y}-\left(\frac{D_z}{R_z}\frac{\partial^2 C}{\partial z^2}+\frac{D_y}{R_y}\frac{\partial^2 C}{\partial y^2}\right)+\wp C=0 \quad (1)$$

ISSN: 2049-3444

Where

$$D_y = \alpha_y v_y + D^*; D_z = \alpha_z v_z + D^* \quad (2)$$

Here, V_y and V_z are the horizontal and vertical conductivities of the medium, D_y and D_z are its horizontal and vertical dispersion coefficients. α_y and α_z are coefficients of dispersivity, while D^* is the diffusion coefficient. R_y and R_z are the equivalent isotropic coefficient of retardation of the contaminant in the medium while $\wp$ is the rate constant of the attendant first order geochemical and allied reactions of contaminant in soil. For example, nitrate undergoes Van Slake reaction in soils .In the model above, Equation (1) is a modified form of the mass balance equation presented by Liang et al (2013).

3.1 The Reduced Flow-Transport Model

To develop a CE/SE computational solution to the mathematical model stated in section 2; we simplify the model by normalizing flow parameters in (1) and (2) with their corresponding scale factors. Following Sudiky and Frind (1982), we employ the physics of the percolation process to decouple Equation (1) to Equations (3) and (4).

$$\frac{\partial}{\partial t}(1+\wp_3 t)C_{(0,z,t)} + \frac{\partial}{\partial z}\left(aC_{(0,z,t)} - Pe_z^{-1}\frac{\partial}{\partial z}C_{(0,z,t)}\right) = 0; \quad 0 \le z \le 1; t \in R. \quad (3)$$

$$\frac{\partial C^{\circ}_{(0,z,t)}}{\partial t} + \wp_1 \frac{\partial C^{\circ}_{(0,z,t)}}{\partial y} = 0; 0^- \le y \le 0^+; t \in R. \quad (4)$$

Here, we have used the concept of dual porosity to introduce the decomposition;

$$C_{(0,z,t)} = C^*_{(0,z,t)} - C^{\circ}_{(0,z,t)} \quad (5)$$

With

$$\frac{\partial C^*_{(0,z,t)}}{\partial y} = \frac{\partial C^{\circ}_{(0,z,t)}}{\partial z} = 0; \text{ and } C^{\circ}_{(0,z,t)} = C_{(y,z,t)}\Big|_{y=0}. \quad (6)$$

a is an arbitrary advection speed introduced in Equation (3) to generalize numerical developments.

The dimensionless groups resulting from derivation equations (3) to (6) are as stated in equation (7)

$$\left\{\begin{array}{l} z = \frac{z}{H};\ y = \frac{y}{\xi};\ T = \frac{R_z H}{u};\ \wp_1 = \frac{2\theta D_y R_z H}{\Delta^2 R_y u};\ \wp_2 = \frac{D_y R_z H}{\Delta^2 R_y u}; \\ \wp_3 = \frac{\wp R_z H}{\Delta^2 R_y u};\ Pe_z = \frac{u_z H}{D_z};\ u = \sqrt{u_z^2 + u_y^2}; \end{array}\right\} \quad (7)$$

Given that u is percolation speed; the characteristic time is of geological time scale i.e. $T \to \infty$ .Hence, using order of magnitude analysis (Hutter and Olunloyo (1982)); the time variant reaction attenuated concentration evolution term $t\wp_3 \frac{\partial C}{\partial t}$ that is introduced to the transport process as a result of equation (3), will vanish.

3.2 Model of Seasonal Applications of Nitrate Fertilizer on Farmlands

Next, we turn attention to the boundary and initial conditions that complement Equations (3), (4), (5) and (6). In order to simulate the Nigerian experience of nitrate pollution of groundwater resources, and deploy a more realistic boundary condition for other contaminant hydrology problems, we want our choice of the contaminant loading function to reflect as much as possible what obtains in normal agricultural practice. Precisely, seasonal loading of fertilizer with a peak concentration C_o is often applied on agricultural soils.

At the upper surface of the soil, the pattern of fertilizer application can be modeled with an integrated Neumann/Dirichelet condition resulting to an exponential decay function of the form $C_o\, e^{-\beta t}$. Such a function accounts for the mode of disappearance of the applied fertilizer on the soil due to plant assimilation, erosion, and percolation. Plant assimilation is equivalent to passive root nutrient uptake identified by Simunek and Hopmans (2009). With repeated seasonal applications, the corresponding nitrate profile on topsoil can then be represented with the periodic signal shown in Figure 3. β is the rate of disappearance of fertilizer, and n is the number of cycles of fertilizer applications. Hatched lines depict anticipated future applications of fertilizer on the farmland under consideration.

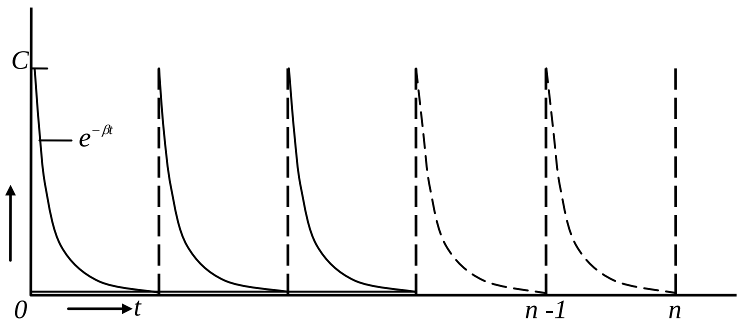

Figure 3: Nitrate Loading Pattern on Farmlands

Clearly, the contaminant loading profile described above has far reaching practical applications in contaminant hydrology. With slight modification, it can be used to handle various types of physical loading conditions that are of concern to hydrologists. As it involves a periodic exponentially decaying function, it gives a better physical representation of what obtains than the *impulsive*, *uniform* and *step function* loadings that have been extensively considered in the literature.

For the avoidance of doubt, a leaking canister of toxic waste in a repository can even be viewed as having a periodic effect on the surrounding aquifer, if for instance a similar canister has leaked in the region in the past or will most probably leak in the future. Such periodicity acts to alter the hydrological properties of the aquifer and the initial concentration of the latest spill.

Essentially our problem now reduces to solving the simultaneous partial differential equations posed in Equations (3), (4), (5) and (6) to obtain the breakthrough curves for the contaminants over time and depth of an aquifer, under the normalized boundary condition:

$$C_{(0,0,t)} = \frac{2C_o(1-e^{-\beta\tau})}{\tau}\left\{\frac{1}{\beta} + \sum_{k=1}^{\infty}\frac{\beta Cos\,\omega t}{\omega^2+\beta^2} + \sum_{k=1}^{\infty}\frac{\omega Sin\,\omega t}{\omega^2+\beta^2}\right\} \quad \text{(8a)}$$

Here, Equation (7a) is a Fourier series representation of the signal in Figure 3. It describes the profile of nitrate on the soil as a function of periodic farming pattern, where $\omega = \frac{2\pi k}{\tau}$; $\tau = 365/T$, $t \in R$.

The complementary boundary conditions in the aquifer along with the loading profile in Equation (7a) are as follows; contaminant concentration decays with depth in the aquifer as defined by

$$c_{(0,\infty,t)} = 0; \quad t \in R \qquad \text{(8b)}$$

The boundary layer between the fracture and matrix has uniform concentration

$$c_{(0,z,t)} = c_{(y,z,t)_{y=0}}; \qquad z > 0, t \in R \quad \text{(8c)}$$

No flux at the matrix centerline i.e. at y = ξ;

$$\left.\frac{\partial c_{(y,z,t)}}{\partial y}\right|_{y=\xi} = 0; \quad 0 \le z \le 1; t \in R \qquad \text{(8d)}$$

3.3 The CE/SE Computational Model

To formulate a CE/SE computational solution for the model developed in Equations (1) through (8), we invoke Gauss divergence theorem, so that the conservation law expressed in equation (3) can be written as;

$$\oint_{S(V)} \vec{g} \bullet d\vec{r} = 0; d\bar{r} = (dz, dt); \qquad \text{(9a)}$$

$$\vec{g} = \left(aC_{(0,z,t)} - Pe_z^{-1}\frac{\partial C}{\partial z}, (1+\wp_3 t)C_{(0,z,t)}\right); \qquad \text{(9b)}$$

To proceed, we integrate Equations (9a&b) by defining $C^*_{(z, t, j, n)}$ and $g^*_{(z, t, j, n)}$ as the discrete values of $C_{(0,z,t)}$ and $\vec{g}_{(0,z,t)}$, at the node $\bullet(j, n)$. This allows us to approximate the numerical distributions of $C^*_{(z, t, j, n)}$ and $g^*_{(z, t, j, n)}$ at mesh points in the neighborhood of node •(j, n) with first order Taylor series. However, in contrast to the stencils of traditional computational schemes, CE/SE mesh points around •(j, n) are staggered such that the difference between the values of *j* and *n* at adjacent nodes alternates between whole numbers and half integers. Detailed layout of CE/SE computational mesh for one and two dimensional solvers can be found in Chang et al, (1996). Using the concept of flux conservation, Equation (8) can be evaluated around a Space-Time rhombus bounded by Δz and Δt to obtain;

$$(\Gamma)_j^n = [\Psi_{adr}]^{-1}\begin{pmatrix} T^- \\ T^+ \end{pmatrix}_j^{n-1/2} \qquad \text{(10)}$$

Here,

$$(\Gamma)_j^n = \begin{pmatrix} C \\ C_z^+ \end{pmatrix}_j^n \qquad \text{(10a)}$$

$$[\Psi_{adr}]^{-1} = \begin{pmatrix} \dfrac{\overset{\vartheta}{-(\vartheta - v)}}{2(1-v^2+\xi)} & \dfrac{\overset{\vartheta}{(\vartheta + v)}}{2(1-v^2+\xi)} \end{pmatrix} \qquad \text{(10b)}$$

$$(T^-)_j^{n-1/2} = (\Phi_{adr}^-)(\Gamma)_{j-1/2}^{n-1/2} \qquad \text{(10c)}$$

$$(T^+)_j^{n-1/2} = (\Phi_{adr}^+)(\Gamma)_{j+1/2}^{n-1/2} \qquad \text{(10d)}$$

$$(\Phi_{adr}^-) = (\vartheta + v \quad \vartheta - v^2 + \xi) \qquad \text{(10e)}$$

$$(\Phi_{adr}^+) = (\vartheta - v \quad -(\vartheta - v^2 + \xi)) \qquad \text{(10f)}$$

$$v = \frac{a\Delta t}{\Delta z};\ \xi = \frac{Pe_z^{-1}\Delta t}{\Delta z^2};\ C_z^+ = \frac{\Delta z}{4}(C_z)_j^n \text{ and}$$
$$\vartheta = (1 + \wp_3 t) \qquad \text{(10g)}$$

Equation (10) is a one-dimensional CE/SE advection dispersion reaction (*adr*) scheme.

4. RESULTS AND DISCUSSION

To facilitate our numerical simulation, we have made use of mean representative values of hydro-geological parameters for homogeneous aquifers as shown in Table 1. These parameters have been corrected for the pattern of annual precipitation on agricultural lands in semi–arid regions of Nigeria. The Peclet numbers and characteristic times for the tabulated aquifers are obtained using a uniform depth to water of 75 meters. This choice is informed by the awareness that depth to water is between 10–150 meters in most localities in Nigeria. Also, we considered an annual cropping cycle of 365 days. This is normalized with the corresponding aquifer's characteristic time to obtain the dimensionless farming period τ

With the awareness that intensive use of fertilizers began in Nigeria in the early 70's, our simulation periods are chosen as 30, 50, and 100 years respectively to characterize the present situation in some National aquifers and predict the trend for the near future. One, two and three fertilizer loading cycles per annum are adopted to depict the perennial nature of grain and vegetable farming in Nigeria especially in the middle belt region, where cropping persists throughout the year along the river basins. This region has for some time been under intensive cultivation with irrigation and fertilizer application.

4.1 Nitrate Breakthrough Curves for Safe Seasonal Loads in Homogeneous Aquifers

Figures 4 and 5 shows the concentration profiles of nitrate in loose clay and fissured limestone aquifers. The figures correspond to one, two and three cycles per annum of fertilizer applications for a period of 30 years without break.

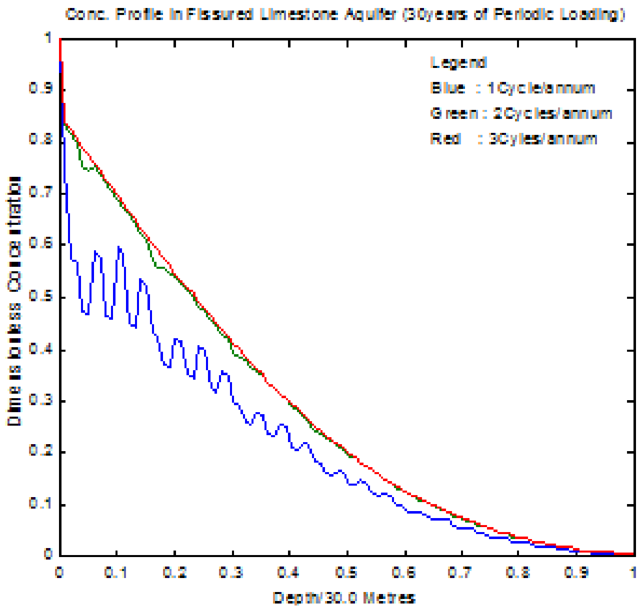

Figure 4

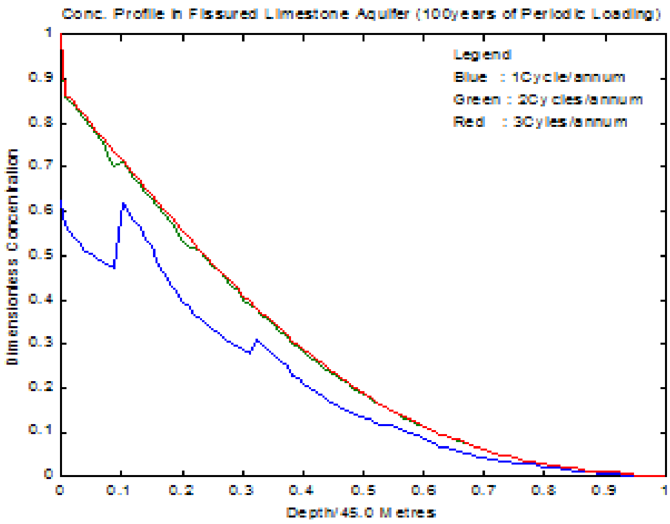

Figure 5

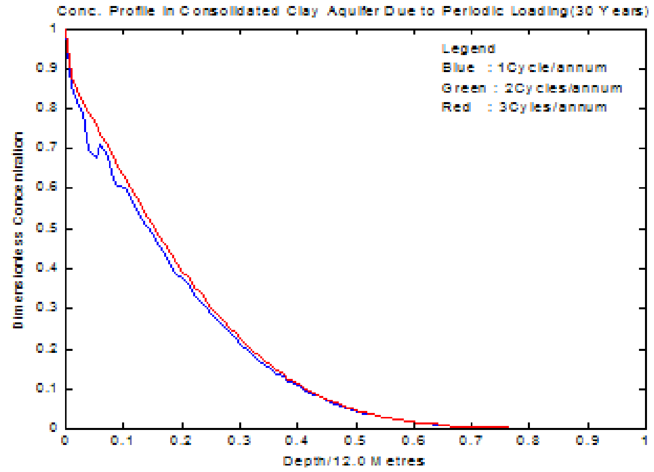

Figure 6

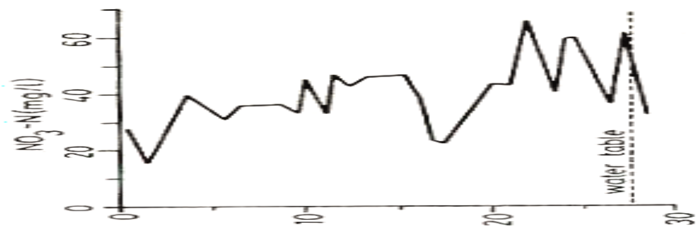

Figure 7a

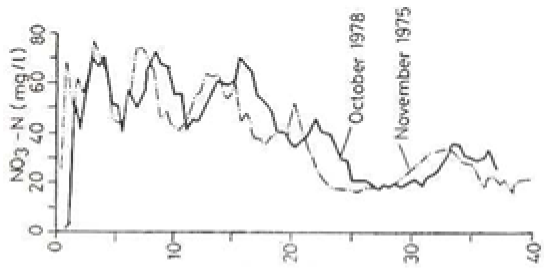

Figure 7b

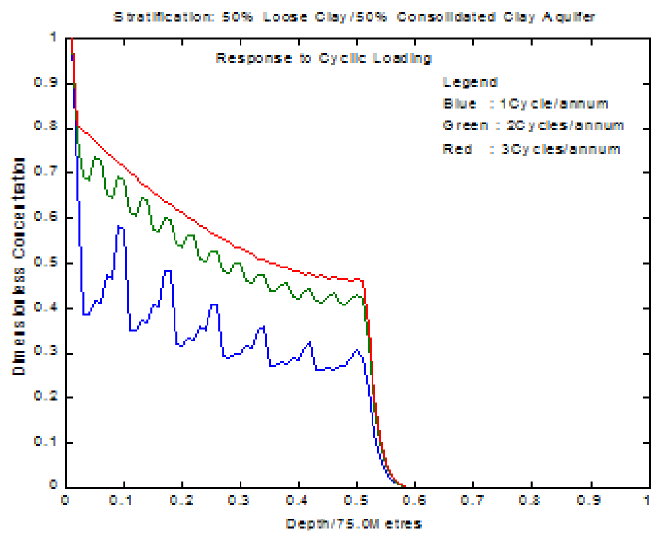

Figure 8

In the same manner, Figure 6 indicates nitrate concentration in consolidated clay aquifer after hundred years of periodic fertilizer applications. Figures 7a and 7b are examples of field observations of nitrate profiles under agricultural lands published independently by Mallick and Banerji, (1981), as well as Moller and Djurhuus (1989). These account for the wavy pattern of our results. To the best of our knowledge, this work is the first analytical/computational scheme to correctly simulate the real pattern of nitrate profiles in groundwater systems as found in the field. In addition, the theoretical basis for the wavy patterns of the concentration profiles is established in Grindrod, (1996).

4.2 Effects of Stratification on Optimal Nitrate Loads

Figure (8) represents the response of a 50% Loose/50% Consolidated Clay system to 1, 2 and 3cycles/annum of periodic loading over 50years duration. Similarly, Figure (9) shows the effect duration of loading on nitrate breakthrough curves in Loose Clay/ Consolidated Clay system. On the other hand, Figure (10) illustrates the effects of composition of the geological log on the breakthrough curves of periodic signals in a stratified aquifer exposed to two cycles per annum loading of the contaminant for 50years.

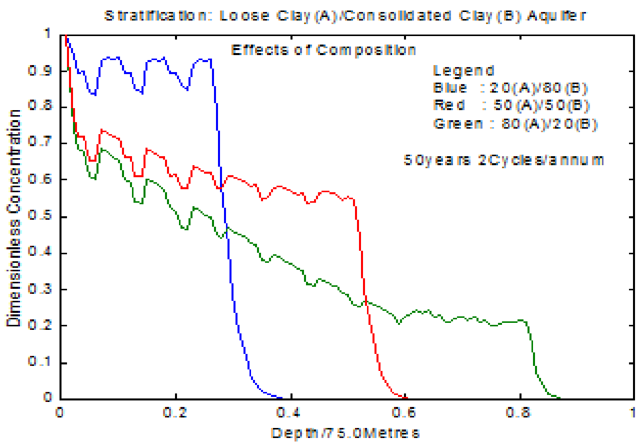

Figure 9

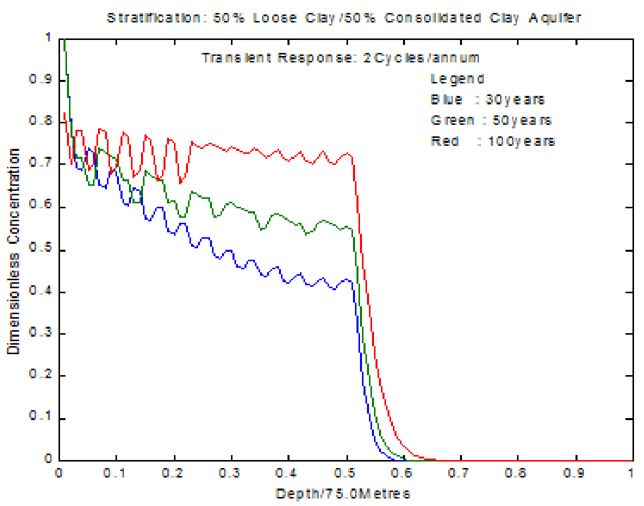

Figure 10

4.3 Prescription of Safe Seasonal Nitrate Load on Homogeneous Aquifers

From Figures 4, 5, and 6, we deduce the optimum loads and frequencies of application nitrate fertilizer on farmlands in the neighborhood of homogeneous aquifers typified by fissured limestone, sand alluvium, and clay formations. For a given number of seasons, these optimal seasonal loads of nitrate ensure that the quality of harbored freshwater at specified depths in these formations meets the WHO standard of 10ppm maximum of nitrate concentration in potable water. Tables 2, 3, 4 and 5 display some of the information embedded in the figures above for the purpose of establishing the optimum seasonal load and frequency of loading for these aquifers using test loads of 50ppm, 100ppm and 150ppm of nitrate on soil surface to characterize mild, moderate, and heavy loads of fertilizer. Similarly, the simulated one, two and three cycles of loading per annum represent low, medium and high frequencies of loading.

Clearly, Table 2 shows that the optimum dosage of nitrate fertilizer applied at the rate of 1 cycle per annum, for a period of thirty years on fissured limestone aquifer with wells deeper than 15meters depth is 50ppm. Consequently, water extracted from wells with depths less than 15meters in this formation should be deployed to irrigation, washing and allied purposes. Within the same time frame, water wells with depths lower than 20meters within the formation can tolerate more than two cycles of 50ppm per annum, or one, two and three cycles of 100ppm. The 150ppm load can only be applied once in a year, otherwise wells in the formation must be deeper than 25meters.

In the case of sand alluvium (Table 3) only 20meters and deeper wells can support one and two cycles of 50ppm loads per annum. Higher combinations of test loads and loading frequencies demand that wells should be at least 25meters deep. However, Table 4 reveals the high capacity of the consolidated clay formation and its relative insensitivity to the frequency of loading. All wells in this formation with depths up to 6meters and above will safely accommodate every combination of test load and frequency considered.

Table 5 illustrates the effects of duration of loading on the determination of optimal seasonal loads. After hundred years, the 50ppm load is applicable in all seasons provided the minimum depth to drinking water is 22.5meters. It is also shown that the difference between medium and high frequencies of fertilizer application is normalized on the long run. So that for higher loads and lower cycle times, nitrate concentrations of 100ppm and 150ppm are acceptable in the formation if the minimum depth to water is 30 meters.

4.4 Prescription of Safe Seasonal Nitrate Loads on Heterogeneous Aquifers

The effect of stratification in a 75meters deep aquifer comprising of equal depths of loose and consolidated clay formations on the optimal seasonal loads of nitrates as shown in Figure 8 is highlighted in Table 6.For all possible combinations of test loads and frequencies considered in our simulation, water tapped from lined wells with bottoms in the lower consolidated clay formations meets the WHO standard. However, the applied nitrate is stored within the loose clay formation, hence wells within this layer are best tapped for irrigation and other ancillary uses.

On the other hand Table 7 expounds the effect of the loading history on the nitrate bearing capacity of the 50%Loose Clay/50%Consolidated clay aquifer described above. Apparently, the pollutant is stored in the loose clay layer for all amplitudes and frequencies of loading. Consequently, only water wells with bottoms within the upper layer are polluted. Lined wells penetrating the consolidated clay formation are significantly protected from all the intensities and rate of loadings considered.

Table 8 derives from Figures 9, 10 and direct computation. It analyses the effects of composition, order of stratification, and time duration on the optimal seasonal nitrate loads. Increasing the proportion of loosed clay on the upper layer to 80% gives the result that only the two cycles per annum 50ppm load is tolerable for lined wells with bottom at the interface between the layers. The table also shows the significant improvement in the tolerability that attends swapping the order of layers of the 50%Loose Clay/ 50% Consolidated Clay Aquifer. Furthermore, the table describes the robustness of 50% Consolidated Clay/50%Loose Clay aquifer to increasing duration of loading. The observed concentration attenuation in the latter type of formation arrangement is consistent with the results of Xiuha et al (2012).

5. CONCLUSIONS

In recognition of the importance of protecting groundwater reserves, we have developed a computational model that correctly simulates the fate of nitrate (and other aqueous contaminants) as it is transported through farmlands to pollute underlying freshwater reservoir. It has been established that the optimum intensity and frequency of nitrate fertilizer application on farmlands that guarantee the integrity of underlying freshwater aquifer depends on the geological profile of the soil in the neighborhood of the farmland and the history of contaminant loading. Furthermore, this model has been applied to assess the present levels of contamination of some water bearing formations found in Nigeria. Specifically, the model has been employed to formulate optimal seasonal loads of nitrogen-based fertilizers on farmlands for the security of groundwater quality for rural dwellers in developing countries. By extension, this model can be used to locate geological repository for spent nuclear fuels and other toxic contaminants. It is also possible to generate manuals of depth to safe water in various geological regions given the hydro-geological properties of the region as well as the history of contaminant loading on the boundaries of aquifers. Thus, we can provide better guidelines on material handling and waste disposal in regions, especially where the natural freshwater reservoir is prone to contamination. This computational model can also be extended for mineral prospecting and groundwater dating.

REFERENCES

Abbas, H. and Booker, R.J., (1999). Groundwater pollution by organic compounds: A two dimensional analysis of contaminant transport in stratified porous media with multiple sources of non-equilibrium partitioning. *International Journal of Numerical Methods in Geomechanics*, 23, 1717 - 1732.

Chang, S. Wang, X. and Chow, C., (1999). The space - time conservation element and solution element method: A new high resolution and genuinely multidimensional paradigm for solving conservation laws. *Journal of Computational Physics*, 156, 89-136.

Deborah, C. and Richard, H., (1990). *Global Freshwater Quality; A First Assessment.* Blackwell Reference, for W.H.O./ U.N.E.P.

Ekkehard, H., (1998). *Modelling Density- Driven Flow in Porous Media*. Springer-Verlag Berlin.

Grindrod, P. (1996). *The Theory and Applications of Reaction Diffusion Equations: Patterns and Waves*. Oxford Applied Mathematics and Computing Series, Clarendon Press. Oxford

Guler, Cuneyt, Thyne, and Geoffred D (2004). Delineation of hydro-chemical facies distribution in regional groundwater system by means of fuzzy c-mean clustering. Water Resour. Res. Vol. 40, No 12, W12503.

Hutter, K. and Olunloyo, V.O.S., (1980). On the distribution of stress and velocity in an ice strip, which is partly sliding over and partly adhering to its bed, by using a Newtonian viscous approximation. *Proc., R., Soc*., London, A373, 385-403.

Jack R.E, Stuart A. R. (2000). Can we predict subsurface mass transport? *Environmental Science and Technology*. Vol. 34, No 18, pp 4010 – 4017.

Kaown D. et al (2009), Identification of nitrate and sulfate sources in groundwater using dual stable isotopes approaches for an agricultural area with different land use(Chuchem and eastern Korea). Agricultural, Ecosystem and Environment. 132, 223-231

Langenegger, O., (1981). High nitrate concentration in shallow aquifers in rural area of central Nigeria, caused by random deposit of domestic refuse and excrement. *In: Quality of Groundwater; Studies in Environmental Sciences.* Elsevier, Amsterdam 17,135-140.

Mallick, S. and Banerji, S., (1981). Nitrate pollution of groundwater as a result of agricultural development in Indoganga Plain, India. *Quality of Groundwater; Proceeding of International Symposium.* 23 –28 March, Noordwijkerhout, Netherlands

Moller, H.E. and Djurhuus, J. (1997). Nitrate leaching as influenced by soil tillage and catch crop. *Soil & Tillage Research* 41, 203-219.

Park, Y. J., Sudiky, E. A., McLaren, R. G.and Sykes, J. F. (2004) Analysis of hydraulic tracer response tests within moderately Fractured Rock based on Transition Probability Geostatical Approach. Water Resour. Res. Vol. 40, No 12, W12404.

Xiuha Liu, Shijun Sun, Peng Ji and Jirka Simunek (2012), Evaluation of historical nitrate sources in groundwater and mpact of current irrigation practices on groundwater quality .Hydrological Science Journal

Yan Liang, Scott A. Bradford, Jiri Simunek, Harry Vereecken and Erwin Klummp (2013) Sensitivity of the transport and retention of stabilized silver nano particles to physico chemical factors. Water Research (47), 2572-2582

Young, K. et. al., (1995). Nitrate Risk Assessment Using Fuzzy-set Approach. *Journal of Environmental Engineering*, 121,3, 245-256.

Table 1: Hydro Geological Parameters

Formation	**Conductivity** *(V)*	**Dispersivity** (D_z)	**Pe**$_z$	T	t	Δt	**Decay Const.**(β)
Silty Sand	$9.6x10^{-4}$	0.45	0.16	$7.8x10^{4}$	$7.8x10^{4}$	$4.6x10^{-3}$	1390
Loose Clay	$9.6x10^{-5}$	0.053	0.14	$7.8x10^{5}$	$4.6x10^{-2}$	$4.6x10^{-4}$	14900
Consolidated Clay	$9.6x10^{-6}$	$2.3x10^{-4}$	3.13	$7.8x10^{6}$	$4.6x10^{-3}$	$4.6x10^{-}$	60800
Fissured Limestone	$9.6x10^{-5}$	$7.5x10^{-3}$	0.96	$7.8x10^{5}$	$4.6x10^{-1}$	$4.6x10^{-5}$	99000
Limestone	$9.6x10^{-6}$	$2.3x10^{-4}$	3.13	$7.8x10^{6}$	$4.6x10^{-3}$	$4.6x10^{-6}$	58900
Sandstone	$9.6x10^{-6}$	$3.5x10^{-3}$	0.21	$7.8x10^{6}$	$4.6x10^{-3}$	$4.6x10^{-6}$	23700

Table 2: Prescribed Safe Nitrate Load per Cycle on Limestone Aquifers of Various Depths to Water for 30Years Farming

Frequency	1Cycle/annum						2Cycles/annum						3Cycles/annum					
Depth → ↓ C_0 (ppm)	5m	10m	15m	20m	25m	30m	5m	10m	15m	20m	25m	30m	5m	10m	15m	20m	25m	30m
50	*21.5*	*14.0*	8.0	3.0	1.0	0.0	*28.5*	*19.0*	*10.0*	4.5	1.5	0.0	*30.0*	*20.0*	*10.0*	4.5	1.5	0.0
100	*43.0*	*28.0*	*16.0*	6.0	2.0	0.0	*57.0*	*38.0*	*20.0*	9.0	3.0	0.0	*60.0*	*40.0*	*20.0*	9.0	3.0	0.0
150	*64.5*	*42.0*	*24.0*	9.0	3.0	0.0	*85.5*	*57.0*	*30.0*	*13.5*	4.5	0.0	*90.0*	*60.0*	*30.0*	*13.5*	4.5	0.0

Blue and red fonts indicate safe and *unsafe* loading configurations respectively.

Table 3: Prescribed Safe Nitrate Load per Cycle on Silty Sand Aquifers of Various Depths to Water for 30Years Farming

Frequency	1Cycle/annum						2Cycles/annum						3Cycles/annum					
Depth → ↓ C_0 (ppm)	5m	10m	15m	20m	25m	30m	5m	10m	15m	20m	25m	30m	5m	10m	15m	20m	25m	30m
50	*20.5*	*15.0*	*10.5*	7.0	1.0	0.0	*29.0*	*22.0*	*14.0*	9.5	2.5	0.0	*35.5*	*26.0*	*15.0*	*10.0*	2.5	0.0
100	*41.0*	*30.0*	*21.0*	*14.0*	2.0	0.0	*58.0*	*44.0*	*28.0*	*19.0*	5.0	0.0	*71.0*	*52.0*	*30.0*	*20.0*	5.0	0.0
150	*61.5*	*45.0*	*31.5*	*21.0*	3.0	0.0	*87.0*	*66.0*	*42.0*	*28.5*	7.5	0.0	*106.5*	*78.0*	*45.0*	*30.0*	7.5	0.0

Blue and red fonts indicate safe and *unsafe* loading configurations respectively.

Table 4: Prescribed Safe Nitrate Load per Cycle on Fissured Limestone Aquifers of Various Depths to Water for 100Years Farming

Frequency .	1Cycle/annum						2Cycles/annum						3Cycles/annum					
Depth → ↓ C_0 (ppm)	7.5m	15m	22.5m	30m	37.5m	45m	7.5m	15m	22.5m	30m	37.5m	45m	7.5m	15m	22.5m	30m	37.5m	45m
50	*24.5*	*15.5*	6.5	1.5	0.5	0.0	*31.0*	*24.5*	9.5	2.5	1.0	0.0	*31.0*	*24.5*	9.5	2.5	1.0	0.0
100	*49.0*	*31.0*	*13.0*	3.0	1.0	0.0	*62.0*	*49.0*	*19.0*	5.0	2.0	0.0	*62.0*	*49.0*	*19.0*	5.0	2.0	0.0
150	*73.5*	*46.5*	*19.5*	4.5	1.5	0.0	*93.0*	*73.5*	*28.5*	7.5	3.0	0.0	*93.0*	*73.5*	*28.5*	7.5	3.0	0.0

Blue and red fonts indicate safe and *unsafe* loading configurations respectively.

Table 5: Prescribed Safe Nitrate Load per Cycle on Consolidated Clay Aquifers of Various Depths to Water for 30Years Farming

Frequency	1Cycle/annum	2Cycles/annum	3Cycles/annum

Depth → / C_o(ppm) ↓	2m	4m	6m	8m	10m	12m	2m	4m	6m	8m	10m	12m	2m	4m	6m	8m	10m	12m
50	*23.50*	8.00	1.50	0.25	0.00	0.00	*24.50*	8.00	1.50	0.25	0.00	0.00	*24.50*	8.00	1.50	0.25	0.00	0.00
100	*47.00*	16.00	3.00	0.50	0.00	0.00	*49.00*	*16.00*	3.00	0.50	0.00	0.00	*49.00*	16.00	3.00	0.50	0.00	0.00
150	*70.50*	24.00	4.50	0.75	0.00	0.00	*73.50*	*24.00*	4.50	0.75	0.00	0.00	*73.50*	24.00	4.50	0.75	0.00	0.00

Blue and red fonts indicate safe and *unsafe* loading configurations respectively.

Table 6: Effects of Farming Frequency on Nitrate Loads for Equally Stratified Loose Clay/ Consolidated Clay Aquifer for 50Years Farming

Frequency	1Cycle/annum						2Cycles/annum						3Cycles/annum					
Depth → / C_0 (ppm) ↓	5m	15m	30m	45m	60m	75m	5m	15m	30m	45m	60m	75m	5m	15m	30m	45m	60m	75m
50	*22.5*	*16.0*	*14.5*	0.0	0.0	0.0	*32.5*	*26.5*	*23.0*	0.0	0.0	0.0	*37.0*	*30.0*	*25.0*	0.0	0.0	0.0
100	*45.0*	*32.0*	*29.0*	0.0	0.0	0.0	*65.0*	*53.0*	*46.0*	0.0	0.0	0.0	*74.0*	*60.0*	*50.0*	0.0	0.0	0.0
150	*67.5*	*48.0*	*43.5*	0.0	0.0	0.0	*97.5*	*79.5*	*69.0*	0.0	0.0	0.0	*111.0*	*90.0*	*75.0*	0.0	0.0	0.0

Blue and red fonts indicate *safe* and *unsafe* loading configurations respectively.

Table 7: Effects of Farming Duration on Two Cycle per Annum Nitrate Loads for Equally Stratified Loose Clay/ Consolidated Clay Aquifer

Duration	30Years						50Years						100Years					
Depth → / C_o(ppm) ↓	5m	15m	30m	45m	60m	75m	5m	15m	30m	45m	60m	75m	5m	15m	30m	45m	60m	75m

50	34.0	26.5	24.0	0.0	0.0	0.0	34.0	31.0	30.0	0.0	0.0	0.0	39.0	37.5	37.0	0.0	0.0	0.0
100	68.0	53.0	48.0	0.0	0.0	0.0	68.0	62.0	60.0	0.0	0.0	0.0	78.0	75.0	74.0	0.0	0.0	0.0
150	102.0	79.5	72.0	0.0	0.0	0.0	102.0	93.0	90.0	0.0	0.0	0.0	117.0	112.5	111.0	0.0	0.0	0.0

Blue and red fonts indicate *safe* and *unsafe* loading configurations respectively.

Table 8: Effects of Geologic Profiles on Prescribed Safe Nitrate Loads in Stratified Clay/Consolidated Clay Aquifer

Composition	80(A)/20(B) ; 50Years; 2Cycles/annum						50(B)/50(A) 50Years; 2Cycles/annum						50(B)/50(A) 100Years; 3Cycles/annum					
Depth → / C_o(ppm) ↓	5m	15m	30m	45m	60m	75m	5m	15m	30m	45m	60m	75m	5m	15m	30m	45m	60m	75m
50	30.0	25.5	23.5	11.0	9.5	0.0	12.0	1.5	0.0	0.0	0.0	0.0	15.6	1.73	0.00	0.00	0.00	0.0
100	60.0	51.0	47.0	22.0	19.0	0.0	24.0	3.0	0.0	0.0	0.0	0.0	31.2	3.45	0.00	0.00	0.00	0.0
150	90.0	76.5	70.5	33.0	28.0	0.0	36.0	4.5	0.0	0.0	0.0	0.0	46.8	5.12	0.00	0.00	0.00	0.0

Blue and red fonts indicate *safe* and *unsafe* loading configurations respectively.